Ab Initio Study of Structure and Spectra of MnH_2, MnH_2^-, and MnH_3

Nikolai B. Balabanov and James E. Boggs*

Institute for Theoretical Chemistry, Department of Chemistry and Biochemistry, The University of Texas at Austin, Austin, Texas 78712

Received: February 18, 2002; In Final Form: May 7, 2002

Molecules of manganese hydrides MnH_2, MnH_2^-, and MnH_3 were studied using large basis sets up to spdfg quality and the coupled cluster technique for the treatment of electron correlation. Both MnH_2 and MnH_2^- have linear equilibrium structures in their high spin ground electronic state, the MnH_2^- molecule having a rather flat bending potential. The MnH_3 molecule is Y-shaped with valence angle $\alpha(H-Mn-H) = 44.6°$ in the $^5B_2$ ground electronic state due to the strong Jahn−Teller distortion of the trigonal planar structure. The harmonic vibrational frequencies, IR intensities, and the relative energies of excited states were calculated. Fundamental vibrational wavenumbers and electron affinity were also found for MnH_2. The results are compared with available spectroscopic data.

Introduction

Manganese dihydride has been the subject of several experimental studies.[1−4] The ground-state properties of the MnH_2 molecule were also examined in previous theoretical studies[5−7] by the CISD(Q), CASSCF, and B3LYP methods. Authors of the spectroscopic studies[1,2] suggested a bent structure for MnH_2. In the theoretical studies[5,7] the molecule was found to be linear. There have been no theoretical predictions of the equilibrium structure of manganese trihydride. The negative ion of manganese dihydride was studied by laser photoelectron spectroscopy,[4] but no high level ab initio calculations of MnH_2^- have been published to our knowledge.[8]

The goals of this work were (1) to calculate the properties of manganese dihydride that have not been studied theoretically, such as the vibrational spectrum, relative energies of excited states, and electron affinity, and (2) to determine the structure and spectra of manganese trihydride. The calculations were performed at a high ab initio level using the coupled cluster technique for treatment of electron correlation along with large basis sets.

Computational Details

The calculations were carried out using the local version of the ACES II program.[9] Several theoretical methods were used: coupled cluster singles and doubles level (CCSD) augmented with a perturbative correction for connected triple excitation (CCSD(T));[10,11] the equation-of-motion coupled cluster method for treatment of excited states in singles and doubles approximation (EOMEE-CCSD);[12] equation-of-motion method for treating of electron-attached states in singles and doubles approximation (EOMEA-CCSD);[13] equation-of-motion method for treating of ionized states in singles and doubles approximation (EOMIP-CCSD).[14] In the EOMEE-CCSD method the wave function is constructed from appropriate coupled-cluster singles and doubles reference wave functions by the action of a wave operator. The EOMEA-CCSD and EOMIP-CCSD wave functions are generated from the CCSD wave function of the molecular system containing one electron less or more by adding or removing an electron from the system.

Three basis sets were used in our calculations:

DZ-ANO: Mn [21s 15p 10d 6f] → (6s 5p 4d 2f), H [8s 4p] → (3s 2p) − double-ζ atomic natural orbital (ANO) basis sets.[15,16]

TZ-ANO: Mn [21s15p10d 6f 4g] → (8s 7p 5d 3f 2g), H [8s 4p 3d] → (4s 3p 2d) − triple-ζ ANO basis sets.[15,16]

TZ-ANO+: The TZ-ANO basis set expanded by adding diffuse functions to each shell except for g. The exponent of the diffuse function corresponded to the smallest one in the contracted ANO.

The Mn−H distance in linear H−Mn−H and trigonal planar structures were found numerically using a fit of five points. Other structures were optimized using analytical first derivatives.

The quadratic force field and harmonic vibrational wavenumbers were obtained at the CCSD level using analytical second derivatives[17] for MnH_2 with the TZ-ANO basis set and MnH_3 with the DZ-ANO basis set. In all other cases the quadratic force field and harmonic vibrational wavenumbers were calculated numerically using second-order finite differences. The MnH_2 cubic and quartic force constants were calculated by numerical differentiation of analytical second derivatives and the fundamental vibrational frequencies were obtained by a second-order perturbation method.[18]

The vibrational energy levels and wave functions that correspond to the bending mode of MnH_2^- were computed by solving the appropriate two-dimensional Schrödinger equation

$$\left\{\frac{1}{2\mu}(\mathbf{P}_x^2 + \mathbf{P}_y^2) + \mathbf{V}(\sqrt{x^2+y^2})\right\}\Psi(x,y) = E\Psi(x,y) \quad (1)$$

using the discrete variable-finite basis representation (DVR/FBR) approach.[19] In eq 1 the coordinates x, y are projections of the MnH_2 bending on two orthogonal planes and the reduced mass is $\mu = 2m_{Mn}m_H(m_{Mn} + 2m_H)^{-1}$. The bending potential $\mathbf{V}$ was represented by an even-power polynomial, which fits a numerical grid. The points on the grid were obtained by calculation of the energies of bent structures at several values of the valence angle $\alpha(H-Mn-H)$. The details of the numerical technique for solving eq 1 were described in ref 20.

* To whom correspondence should be sent. Fax: 512-471-8696. E-mail: james.boggs@mail.utexas.edu.

10.1021/jp0204399 CCC: $22.00
Published on Web 06/27/2002

TABLE 1: Total Energies (E, au), the Equilibrium Mn−H Distances (R_e, Å), the Harmonic Vibrational Frequencies (ω_i, cm^{-1}) and IR Intensities (A_i, km/mol) in the Ground States of MnH_2 and MnH_2^-

molecule	E	R_e[a]	$\omega_1(\Sigma_g^+)$	$\omega_2(\Sigma_u^-)$	$\omega_3(\Pi_u)$	A_2	A_3	method/basis
MnH_2	−1551.000901	1.7512	1637.1	1616.8	427.5	592.5	926.6	UHF/TZ-ANO
	−1551.647097	1.6923	1714.3	1677.9	444.1	560.9	762.1	SDQ-MBPT(4)/TZ-ANO
	−1551.647295	1.6947	1699.9	1656.7	419.0	587.1	757.5	CCSD/TZ-ANO
	−1551.662879	1.6905	1703.5	1658.3	408.1	573.1	727.2	CCSD(T)/TZ-ANO
	−1551.704396	1.6956	1717.1	1675.7	391.1			CCSD/TZ-ANO+
	−1551.720690	1.6914	1722.1	1682.9	383.4			CCSD(T)/TZ-ANO+
MnH_2^-	−1151.649699	1.6956	1514.7	1429.5	153.7			EOMEA-CCSD/TZ-ANO
	−1151.709701	1.6958	1568.9	1487.9	37.6			EOMEA-CCSD/TZ-ANO+

[a] 1.754 Å with the CISD(Q) method,[5] 1.78 Å by the CASSCF method,[6] 1.691 Å with the B3LYP method[7]

TABLE 2: Relative Energies of Excited Electronic State in MnH_2 and MnH_2^-

molecule	state	r(M−H), Å	ΔE, cm^{-1}	method[b]
MnH_2	$^6\Sigma_g^+$, $(1\pi_g)^2(1\delta_g)^2(5\sigma_g)^1$	1.6905	0	
	$^4B_2$, $(b_2)^1(a_1)^1(a_1)^1$	1.5756[a]	21125	CCSD(T)
	$^6\Sigma_u^+$, $(3\sigma_u)^3(1\pi_g)^2(1\delta_g)^2(5\sigma_g)^2$	1.6593	29803	EOMEE-CCSD
	$^6\Pi_u$, $(3\sigma_u)^3(1\pi_g)^3(1\delta_g)^2(5\sigma_g)^1$	1.6603	35472	EOMEE-CCSD
	$^2\Sigma_g^+$, $(1\pi_g)^4(5\sigma_g)^1$	1.6364	41561	CCSD(T)
	$^2\Sigma_g^+$, $(1\delta_g)^4(5\sigma_g)^1$	1.7029	44365	CCSD(T)
MnH_2^-	$^5\Sigma_g^+$, $(1\pi_g)^2(1\delta_g)^2(5\sigma_g)^2$	1.6959	−528	EOMEA-CCSD
	$^5\Pi_g$, $(1\pi_g)^3(1\delta_g)^2(5\sigma_g)^1$	1.7563	11363	EOMEA-CCSD
	$^5\Delta_g$, $(1\pi_g)^2(1\delta_g)^3(5\sigma_g)^1$	1.7237	11606	EOMEA-CCSD

[a] ∠H−Mn−H = 106.0°. [b] TZ-ANO basis set.

The probabilities of transition in the photoelectron spectra of MnH_2^- were evaluated as the square of the overlap integral

$$R^{ov} = |\int \Psi_{ion,o}(Q)\Psi_{neutral,v}(Q)\, dQ|^2 \qquad (2)$$

where $\Psi_{ion,0}(Q)$ corresponds to the eigenfunction of the ground vibrational level in the negative ion and $\Psi_{neutral,v}(Q)$ is the eigenfunction of the vibrational level of the neutral molecule. The vibrational eigenfunctions were presented as the product of the vibrational wave function for each single mode. The single mode vibrational functions were Hermite's function for the stretching modes. The wave functions corresponding to the bending mode of MnH_2^- were obtained by solving eq 1. The ion and neutral molecule normal coordinates Q were taken as identical due to the almost identical equilibrium structures of these molecules. The overlap integral (2) was computed numerically using the adaptive Monte Carlo procedure.[21]

Results and Discussion

MnH_2. The MnH_2 ground-state total energy, equilibrium parameters, harmonic vibrational frequencies, and IR intensities calculated at several levels of theory for comparison are collected in Table 1. At all levels of theory we found the molecule to be linear. In the leading electronic configuration, single occupied molecular orbitals $1\pi_g$, $1\delta_g$, and $5\sigma_g$ arise from the Mn d-orbitals. All amplitudes (T_1 and T_2) in the CCSD wave function of MnH_2 are less than 0.053, indicating that the single reference methods are appropriate for the molecule.

The results show that there is a strong correlation effect on the Mn−H distance. The distance shortens by 0.0607 Å at the CCSD(T) level compared with the UHF distance, both with the TZ-ANO basis set. The contribution of triple excitations is 0.0042 Å. Similar correlation effects that lead to strong contraction of the metal−hydrogen distance were found in theoretical studies of the chromium hydride molecule.[22] The strong contraction of the Mn−H distance correlates, as would be expected, with a significant increase of the theoretical values of the stretching harmonic vibration frequencies. Expansion of the basis set with additional diffuse functions gives a large contribution to the total energy of MnH_2, but a small (only 0.0009 Å) correction to the value of the Mn−H distance. It also increases slightly the theoretical value for the stretch vibrational wavenumbers and decreases the bending harmonic frequency. The value R_e(Mn−H) = 1.6914 Å found by the CCSD(T)/TZ-ANO+ is in excellent agreement with R_e(Mn−H) = 1.691 Å obtained in a recent DFT study.[7]

TABLE 3: Theoretical and Experimental Fundamental Wavenumbers (ν_i, cm^{-1}) in MnH_2

$\nu_1(\Sigma_g^+)$, stretching	$\nu_2(\Sigma_u^-)$, stretching	$\nu_3(\Pi_u)$, bending	method[a]
1591.3	1571.1	423.6	UHF
1666.1	1632.9	427.6	SDQ-MBPT(4)
1644.8	1608.6	406.2	CCSD
1646.5	1608.9	394.5	CCSD(T)
	1594.0		MI IR (Ar)[b]
	1591/1565	375/366	MI IR (Xe)[c]

[a] TZ-ANO basis set. [b] Reference 1. [c] Reference 3.

The relative energies and equilibrium parameters of several excited states of MnH_2 are given in Table 2. All of them lie more than 20 000 cm^{-1} higher than the ground state. The first excited state $^4B_2$, $(b_2)^2(b_1)^1(a_1)^1(a_1)^1$ has a bent equilibrium structure with ∠H−Mn−H = 106.0°. In the leading electronic configuration of the $^4B_2$ state the doubly occupied b_2 orbital results from a strong mixture of the manganese $3d_{zx}$ orbital with the hydrogen 1s atomic orbitals.

The two IR active MnH_2 vibrational frequencies have large intensities (see Table 1). Anharmonic corrections to all vibration wavenumbers are negative and amount to ∼3% (see Table 3). In the previous theoretical study, the authors[5] noted that the bending potential of MnH_2 is relatively flat. Indeed, according to our calculation at the CCSD/TZ-ANO+ level the energy of the bent structure with α(H−Mn−H) = 150° is only ∼2.6 kcal/mol higher the linear H−Mn−H one (cf. 3.0 kcal/mol obtained in ref 5). However, approximation of the MnH_2 bending potential with an even-power polynomial showed that the quadratic term gives by far the largest contribution and the potential is nearly harmonic, which is no indication of a flat area near the minimum. Therefore we can expect the perturbation theory method to give a reasonable value for the $\nu_3(\Pi_u)$ fundamental.

The observed bands in the IR spectrum assigned to MnH_2 were reported in two spectroscopic studies.[1,3] The authors of the earlier study reported a single band at 1594.0 cm^{-1} in the IR spectrum of MnH_2 in Ar matrix, which was due to the antisymmmetric stretch ν_2. The theoretical value for ν_2 is only 14.9 cm^{-1} higher. This small discrepancy is reasonable if one takes into account the possible residual errors of the theoretical methods due to the incompleteness of basis sets and neglect of correlation effects of higher orders, as well as neglecting in our calculation the effect of the Ar matrix atom on the structure of MnH_2. In a subsequent spectroscopic study the authors[3] reported a more complex structure of the IR spectrum of the MnH_2 molecules trapped in solid xenon. Overall, four absorptions at 1591, 1565 and 375, 366 cm^{-1} were found in the spectrum.[3] The authors explained the result by postulating the presence of two species: **A**, which absorbs at 1591 and 375 cm^{-1}, and **B**, which absorbs at 1565 and 366 cm^{-1}. In their experiment, species **B** was favored. However, the ν_2 and ν_3 fundamentals calculated here are in accord with the wavenumbers of their less abundant species **A**. The identity of their spectra for **B** is not evident.

Another property of MnH_2 obtained experimentally, the electron affinity, was found from the laser photoelectron spectrum of the MnH_2^- negative ion in ref 4. Using the CCSD wave function of the MnH_2 ground state, we calculated the energies of several possible ionic states by the equation-of-motion−electron-attachment method and only one ionic state was found to lie below the energy of the neutral MnH_2 molecule (see Table 2). This state results from adding an electron to the singly occupied $5\sigma_g^+(d_{r^2-z^2})$ orbital. It should be noted here that the direct computation of the $^5\Sigma_g^+$, $(1\pi_g)^2(1\delta_g)^2(5\sigma_g)^2$ by the CCSD and CCSD(T) methods is not reliable due to a large spin contamination in the UHF reference function. The other electronic states of MnH_2^- lie more than 11 000 cm^{-1} higher than the ground-state energy of the neutral species.

The calculation showed that MnH_2^- is linear with a small value of the bending frequency. Thus both manganese dihydride and its negative ion have linear structures in their ground states and the Mn−H distances in the two species differ only by 0.0001 Å at the singles and doubles level. The energies of several bent structures of MnH_2^- were calculated with the TZ-ANO+ basis set. Approximation of the energies by an even-power polynomial showed that in contrast to neutral MnH_2 the negative ion bending potential is very flat (see Figure 1) and the obtained points cannot be described only with a second degree term. Therefore the harmonic approximation is not appropriate for finding the vibrational energy levels and corresponding vibrational wave functions. The vibrational levels corresponding to the bending mode, as found by solving the Schrödinger equation, are presented in Table 4. We estimated the probabilities of several transitions from the ground vibrational state in the negative ion to vibrational states in manganese dihydride (Table 5). As expected, the (0,0,0) → (0,0,0) transition has the largest intensity.

Our result is in qualitative agreement with conclusions of experiment.[4] In ref 4 the lack of vibrational structures in the photoelectron spectrum of MnH_2^- was explained by the suggestion that manganese dihydride and its ion likely have similar geometrical structures. With the TZ-ANO+ basis set the adiabatic electron affinity $EA_e = E(MnH_2) - E(MnH_2^-) =$ 0.144 eV, the ZPVE correction is 0.050 eV, and the total electron affinity $EA_0 = 0.194$ eV. This value is much less than the 0.444 ± 0.016 eV obtained by experiment.[4] We recalculated the difference $E(MnH_2) - E(MnH_2^-)$ in a single point calculation with introducing additional diffuse functions to the TZ ANO+ basis set on Mn to each shell except g and replacing the TZ ANO+ basis on H with an aug-cc-pvqz basis set.[23] The result was 0.156 eV. Further investigations of the influence of the basis set, especially on the Mn atom, and of correlation effects of higher order on the theoretical value of the MnH_2 electron affinity are necessary.

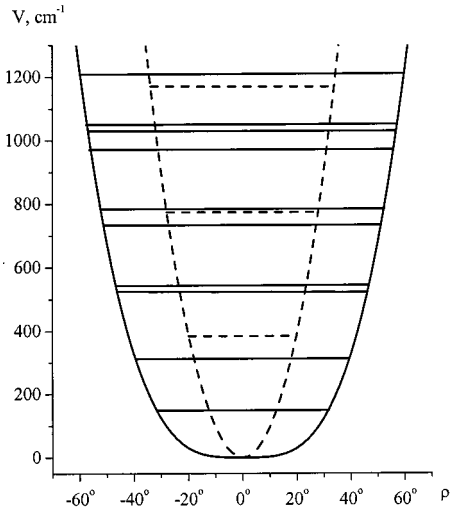

Figure 1. Energy of MnH_2^- and MnH_2 (in dashed line) as functions of angle $\rho = 180° - \alpha(H-Mn-H)$ along with corresponding vibrational levels as found with eq 1.

TABLE 4: Vibrational Energy Levels for the Bending Mode in MnH_2 and MnH_2^-

		energy	
level	degeneracy	MnH_2	MnH_2^-
0	1	384.3	149.2
1	2	774.4	312.7
2	2	1169.7	523.9
3	1	1175.0	541.6
4	2	1569.7	731.7
5	2	1579.6	776.3
6	2	1974.3	972.4
7	2	1988.5	1027.7
8	1	1993.2	1052.4
9	2	2383.4	1212.6
10	2	2401.7	1274.8

TABLE 5: Theoretical Probabilities of Transitions in Photoelectron Spectra of MnH_2^-

transition	probability	ΔE, eV
0,0,0 → 0,0,0	0.833	0.194
0,0,0 → 0,0,3	0.136	0.292
0,0,0 → 0,0,8	0.016	0.393

MnH_3. The possible experimental evidence for existence of the manganese trihydride molecule was reported in ref 1: the authors reported lines in the ESR spectrum of the Mn + H_2 system, which could be caused by the presence of the MnH_3 molecules.

We have calculated the structure of the lowest quintet, triplet, and singlet electronic states of MnH_3 at the trigonal planar (D_{3h}) structure. Three electronic states could be possible candidates for the MnH_3 lowest quintet state. These states result from the distribution of 4 electrons in 5 molecular orbitals: $1e''(d_{zx}, d_{zy})$, $5a_1'(d_{z^2-r^2})$, and $4e'(d_{xy}, d_{x^2-y^2})$. The EOMIP method allows one to calculate the total energies of these states by using the reference CCSD wave function of the $^6A_1'$, $(1e'')^2(5a_1')^1(4e')^2$ state of the negative ion MnH_3^- and removing one electron. The results are presenting in Table 6. The lowest quintet state

TABLE 6: Total Energies (E, au) and Optimal R_e(Mn−H) Distances (Å) of MnH_3 in Several Electronic States at Planar Trigonal (D_{3h}) Structure

state	R_e(Mn−H)	E	method[a]
$^5E'$, $(1e'')^2(a_1')^1(3e')^1$	1.6695	−1152.154865	EOMIP−CCSD
$^3E''$, $(1e'')^3(a_1')^1$	1.5584	−1152.085288	EOMEE-CCSD
$^1A_1'$, $(1e'')^4$	1.5482	−1152.057636	CCSD
$^5A_1'$, $(1e'')^2(a_1')^1(3e')^1$	1.7152	−1152.052175	EOMIP−CCSD
$^5E''$, $(1e'')^2(a_1')^1(3e')^1$	1.6244	−1152.013067	EOMIP−CCSD

[a] TZ-ANO basis set.

is the $^5E'$ degenerate state. The other two quintet states calculated here lie higher in energy than the $^5E'$ state.

The energies of the lowest D_{3h} singlet and triplet states were calculated by the EOMEE-CCSD method using the CCSD wave function of the $(1e'')^4$, $^1A_1'$ state as a reference. The lowest one was the triplet $(1e'')^3(5a_1')^1$, $^3E''$ state, which lies 6069 cm^{-1} below the energy of the $(1e'')^4$, $^1A_1'$ state, which is the lowest singlet state.

Thus the quintet $^5E'$ state lies much below other electronic states at the D_{3h} nuclear configuration. According to the Jahn−Teller theorem[24,25] the degenerate $^5E'$ state is the conical intersection of two electronic states, which correspond to the molecular configurations of symmetry lower than D_{3h}. With a deformation of the trigonal planar structure to the T-shaped or Y-shaped formation of C_{2v} symmetry, the $^5E'$ electronic state splits into the $^5A_1$ and $^5B_2$ states, the energies of which are significantly decreased with respect to the energy at the D_{3h} configuration.

The full C_{2v} optimization of molecular structures of the $^5A_1$ and $^5B_2$ states was carried out with DZ-ANO and TZ-ANO basis sets without g-functions, and the TZ-ANO($-g$) basis was extended by diffuse functions (see Table 7and Figure 2). The presence of g-functions in the TZ-ANO basis sets resulted in spin-contamination in the MnH_3^- UHF reference wave function for the C_{2v} molecular structures, which are strongly deformed from the trigonal planar configuration. The addition of diffuse functions gave a little correction on the Mn−H optimal distance at the D_{3h} structure but resulted in significant contraction of the internuclear distances and large changes of valence angles for distorted C_{2v} structures. The $^5B_2$ state has a Y-shaped equilibrium structure and corresponds to one of three minima on the total Jahn−Teller surface of the molecule. The optimal geometrical structure of the $^5A_1$ state is T-shaped and represents one of three barriers on the Jahn−Teller surface. The structure of MnH_3 differs from its analogue MnF_3: in contrast to MnH_3, the MnF_3 molecule has three T-shaped minima on its Jahn−Teller surface separated by three Y-shaped barriers.[26] The distortion of the trigonal planar structure and correspondently the Jahn−Teller stabilization energy in MnH_3 are larger than in the MnF_3 case.

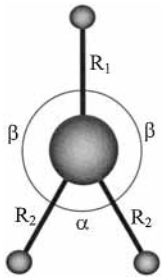

Figure 2. Internal coordinate notation for MnH_3 of C_{2v} symmetry

Taking into account that the minima on the MnH_3 Jahn−Teller surface are isolated due to both the high magnitude of the barriers and the high relative energy of the conical intersection point at the trigonal planar structure, the lowest vibrational levels of the molecule can be estimated within the adiabatical approximation. The harmonic frequencies of Y-shaped MnH_3 are presented in Table 7. The corresponding bands in the IR spectrum should have smaller intensities than those attributed to the MnH_2 molecules.

The lowest triplet $^3E''$state at the D_{3h} structure is also subject to the Jahn−Teller effect. However the calculation of energies of configurations slightly deformed from trigonal planar showed that the Jahn−Teller distortion does not exceed a few degrees from $\alpha(H-Mn-H) = 120°$ in contrast to the case of the quintet $^5E'$ state. This can be explained by the fact that the $1e''(d_{zx}, d_{zy})$

TABLE 7: D_{3h} and C_{2v} Geometrical Parameters, Jahn−Teller Stabilization Energies (ΔE_{JT}) and Barriers (h_{JT}), Harmonic Vibration Frequencies, and IR Intensities of MnH_3 in the Ground Electronic State

state	parameter[a]	DZ-ANO	TZ-ANO($-g$)[b]	TZ-ANO+($-$g)[b]
$^5E'$, D_{3h}	R_e(Mn−H), Å	1.6713	1.6699	1.6715
	E, au	−1151.994815	−1152.103260	−1152.158897
$^5B_2$, C_{2v}	R_1(Mn−$H_{(1)}$), Å	1.6943	1.6965	1.6831
	R_2(Mn−$H_{(2)}$), Å	1.6664	1.6641	1.6488
	$\alpha(H_{(2)}-Mn-H_{(3)})$, deg	59.7	57.4	44.6
	ΔE_{JT},[c] cm^{-1}	6988	7427	7647
	$\omega(A_1)$, cm^{-1}	1698 (271)	1671	1701
	$\omega(A_1)$, cm^{-1}	1458 (127)	1376	1474
	$\omega(A_1)$, cm^{-1}	489 (9)	523	413
	$\omega(B_2)$, cm^{-1}	1595 (8)	1591	1703
	$\omega(B_2)$, cm^{-1}	381 (240)	425	483
	$\omega(B_1)$, cm^{-1}	393 (293)	373	388
$^5A_1$, C_{2v}	R_1(Mn−$H_{(1)}$), Å	1.6422	1.6375	1.5973
	R_2(Mn−$H_{(2)}$), Å	1.6780	1.6784	1.6602
	$\beta(H_{(2)}-Mn-H_{(3)})$, deg	96.7	96.2	91.2
	ΔE_{JT},[d] cm^{-1}	5362	5698	5818
	h_{JT},[e] cm^{-1}	1626	1729	1830
	$\omega(A_1)$, cm^{-1} (A, km/mol)	1719 (40)	1695	1784
	$\omega(A_1)$, cm^{-1}	1475 (54)	1410	1585
	$\omega(A_1)$, cm^{-1}	531 (301)	552	550
	$\omega(B_2)$, cm^{-1}	1687 (775)	1630	1725
	$\omega(B_2)$, cm^{-1}	473i (229)	413i	343i
	$\omega(B_1)$, cm^{-1}	442 (320)	524	571

[a] Notations of internal coordinates are found in Figure 2. [b] Mn g-function was excluded. [c] Difference in energy between the $^5E'$ and $^5B_2$ states. [d] Difference in energy between the $^5E'$ and $^5A_1$ states. [e] Difference in energy between the $^5B_2$ and $^5A_1$ states.

orbitals are orthogonal to the plane of the molecule and distribution of an electron cannot cause big changes in the valence angles and the Mn−H distance compared to the JT distortion in the $^5E'$ state, where one electron is distributed between two $e'(d_{x^2-y^2}, d_{xy})$ orbitals that are located along the plane of the molecule. The MnH_3 lowest singlet state, the reference $(1e'')^4$, $^1A_1'$, is unstable at the trigonal planar structure. Full optimization at the CCSD/TZ-ANO level leads to a pyramidal equilibrium structure with the valence angle α_e(H−Mn−H) = 106.0°, R_e(Mn−H) = 1.5371 Å, and a barrier to planarity in 1837 cm^{-1}.

Acknowledgment. This work was supported by a grant from Robert A. Welch Foundation. We are thankful to John Stanton for valuable help.

References and Notes

(1) Van Zee, R. J.; DeVore, T. C.; Willkerson, J. L.; Weltner, W., Jr. *J. Chem. Phys*. **1978**, *69*, 1869.

(2) Van Zee, R. J.; Brown, C. M.; Weltner, W., Jr. *Chem. Phys. Lett.* **1979**, *64*, 325.

(3) Ozin, G. A.; McCaffrey, J. G. *J. Am. Chem. Soc.* **1984**, *106*, 807.

(4) Miller, A. E. S.; Feigerle, C. S.; Lineberger, W. C. *J. Chem. Phys*. **1986**, *84*, 4127.

(5) Demuynck, J.; Schaefer, H. F. *J. Chem. Phys.* **1980**, *72*, 311.

(6) Fujii, T. S.; Iwata, S. *Chem. Phys. Lett.* **1996**, *251*, 150.

(7) Plattes, J. A. *J. Mol. Struct*. **2001**, *545*, 111.

(8) The negative ion of MnH_2 was studied only with the X_α method in: Gutsev, G. L. *Izv. Akad. Nauk SSSR, Ser. Khim*. **1989**, *1*, 81.

(9) Stanton, J. F.; Gauss, J.; Watts, J. D.; Lauderdale, W. J.; Bartlett, R. J. *Int. J. Quantum Chem. Symp*. **1992**, *26*, 879.

(10) Raghavachari, K.; Trucks, G. W.; Pople, J. A.; Head-Gordon, M. *Chem. Phys. Lett*. **1989**, *157*, 479.

(11) Bartlett, R. J.; Watts, J. D.; Kucharski, S. A.; Noga, J. *Chem. Phys. Lett*. **1990**, *165*, 513.

(12) Stanton, J. F.; Bartlett, R. J. *J. Chem. Phys.* **1993**, *98*, 7029 and references therein.

(13) Nooijen, M.; Bartlett, R. J. *J. Chem. Phys.* **1995**, *102*, 3629.

(14) Stanton, J. F.; Gauss, J. *J. Chem. Phys*. **1994**, *101*, 8938.

(15) Widmark, P. O.; Malmqvist, P. A.; Roos, B. O. *Theor. Chim. Acta* **1990**, *77*, 291. The basis sets were obtained from the Extensible Computational Chemistry Environment Basis Set Database, Version 1.0, as developed and distributed by the Molecular Science Computing Facility, Environmental and Molecular Sciences Laboratory, which is part of the Pacific Northwest Laboratory, P.O. Box 999, Richland, WA 99352, and funded by the U.S. Department of Energy. The Pacific Northwest Laboratory is a multiprogram laboratory operated by Battelle Memorial Institute for the U.S. Department of Energy under contract DE-AC06-76RLO 1830. Contact David Feller or Karen Schuchardt for further information.

(16) Pou-Amerigo, R.; Merchan, M.; Nebot-Gil, I.; Widmark, P. O.; Roos, B. O. *Theor. Chim. Acta* **1995**, *92*, 149.

(17) Gauss, J.; Stanton, J. F. *Chem. Phys. Lett.* **1997**, *276*, 70.

(18) Stanton, J. F.; Lopreore, C. L.; Gauss, J. *J. Chem. Phys*. **1998**, *108*, 7190.

(19) Light, J. C.; Hamilton, I. P.; Lill, J. V. *J. Chem. Phys.* **1985**, *82*, 1400.

(20) Balabanov, N. B.; Boggs, J. E. *J. Phys. Chem. A* **2000**, *104*, 7370.

(21) We used the VEGAS routine from: W. H.; Teukolsky, S. A.; Vetterling, W. T.; Flannery, B. P. *Numerical Recipes in C*; Cambridge University Press: Cambridge, U.K., 1992.

(22) Deleeuw, B. J.; Yamaguchi, Y.; Schaefer, H. F. *Mol. Phys*. **1995**, *84*, 1109.

(23) Dunning Jr., T. H. *J. Chem. Phys.* **1989**, *90*, 1007.

(24) Englman, R. *The Jahn−Teller effect*; Wiley: New York, 1972.

(25) Bersuker, I. B.; Polinger, V. Z. *Vibronic Interaction in Molecules and Crystals*, Springer-Verlag: New York, 1989.

(26) Solomonik, V. G.; Sliznev, V. V.; Balabanov, N. B. *Z. Phys. Chem*. **1997**, *200*, 77.